To cite this article: JIAO L Q, ZHANG Q, LI M, et al. Damage characteristics of stiffened plates in typical cabin explosion load [J/OL]. Chinese Journal of Ship Research, 2021, 16(2). http://www.ship-research.com/EN/Y2021/V16/I2/108.

DOI: 10.19693/j.issn.1673-3185.01841

Damage characteristics of stiffened plates in typical cabin explosion load

JIAO Liqi[1], *ZHANG Quan*[2], *LI Mao*[1], *ZHANG Lei*[1], *ZHANG Chunhui*[1]

1 Naval Research Academy, Beijing 100161, China

2 Science and Technology on Reactor System Design Technology Laboratory of NPIC, Chengdu 610213, China

Abstract: [**Objectives**] In order to study the damage characteristics of a typical cabin explosion load on stiffened plates, we divide the explosion load in a cabin into the initial explosive shock wave load and quasi-static air pressure load and use finite element analysis software LS-DYNA to simulate and calculate the damage characteristics of fixed stiffened plates under the explosion load. [**Methods**] In this paper, the deformation characteristics of the stiffened plate under the same impulse and peak load are simulated, and the damage characteristics of the stiffened plate under the initial explosive shock wave load, quasi-static air pressure load, and the combined action of the two loads are analyzed. [**Results**] The results show that when the impulse acting on the stiffened plates is equal and the load action time is less than 0.05 times the vertical first-order natural vibration period, the final deflection value of the stiffened plates is near the maximum value. When the load peaks are equal, there is a saturated impulse value, after which the loading time no longer affects the final deformation of the stiffened plates. [**Conclusions**] The final deformation of stiffened plates under an explosion load in a cabin is not a simple superposition under the action of two loads; the combined effect of the two loads enhances their damage.

Key words: stiffened plate; cabin explosion load; saturated impulse; combined effect; deformation; damage characteristics

CLC number: U661.43

0 Introduction

With the development of anti-ship weapons, the semi-armor-piercing anti-ship missile has become the main attack means to destroy the hull structure of a surface ship. After the warhead has pierced the planking of a cabin and exploded in the cabin, the damage power of the weapon increases greatly, causing not only damage to the ship structure by the shock wave load due to the explosion, but also further damage to the ship cabin structure by the quasi-static air pressure resulted from explosion of the warhead. Through comparison between the damage and deformation of the stiffened plate in the cabin explosion experiment and those under the aerial explosion load, it can be seen that the cabin explosion load is greatly different from the aerial explosion load in the free field. A study on the combined effect of the shock wave load due to the cabin explosion and the quasi-static air pressure is of great significance for the protection of the warship structure and damage assessment.

The study on the characteristics of the cabin explosion load mostly relies on the cabin explosion experiment and numerical simulation of the cabin explosion. Sauvan et al. [1] have studied the generation of the reflected shock wave load in a cabin explosion by simulating the coupling effect of the reflected shock wave resulted from the cabin explosion by providing a grillage structure around the explosion source. Baker [2] has proposed the well-known three-shock-wave equivalence method by

Received: 2019-12-02 **Accepted:** 2020-03-03

Authors: JIAO Liqi, male, born in 1993, master. Research interest: warship explosion impact and protection. E-mail: 1758981315@qq.com

ZHANG Quan, male, born 1994, master. Research interest: warship explosion impact and protection. E-mail: 1013150451@qq.com

***Corresponding author:** ZHANG Quan

downloaded from www.ship-research.com

conducting a series of experiments and theoretical studies based on the features of the explosive shock wave in the cabin, such as high overpressure peak, short action time, and multiple times of reflection. HOU et al. [3] have conducted an experimental study on the cabin explosion with a typical cabin. Their study results indicate that, as affected by the warship structure, besides the shock waves reflected from the walls, among the shock loads to be borne by the grillage structure of the cabin under the cabin explosion, there are convergent shock waves at the cabin corners of which the intensity is far bigger than that of the shock waves reflected from the walls; also, multiple repeated actions of these shock waves exist. KONG et al. [4] have conducted experimental studies on the explosion in a cabin with multi-layer protection structure, and through analysis, the experimental results indicate that the dynamic response of the inner plates of the water chamber has a "secondary loading" phenomenon under the explosion load. FAN et al. [5] have analyzed the propagation characteristics of the cabin explosion load and proposed that a quasi-static pressure zone has been formed in the cabin due to the reflection effect of the shock waves by simulating the typical cabin explosion with the finite element software ANSYS/LS-DYNA. In LR Rules and Regulations for Classification of Ships [6], it is pointed out that the quasi-static air pressure peak is closely related to the ratio of charging to cabin volume. ZHANG et al. [7] and JIN et al. [8] have reached the conclusion that the ratio of charging to cabin volume has the decisive impact on the quasi-static air pressure peak through experiments, and fitted out the empirical formula for calculation of the quasi-static pressure with the experimental data. With the above studies, it can be concluded that the cabin explosion load mainly includes the shock wave load and quasi-static air pressure load if the fragment load is not considered.

Also, some scholars have studied the dynamic response and damage mode of the stiffened plate under the shock wave as well as quasi-static air pressure. YAN et al. [9] have reached the conclusion that the contributing factor for damage is the shock wave from an internal explosion through numerical simulation of the damage under the internal explosion of the anti-ship missile with bulkheads of different thicknesses. YAO et al. [10] have conducted experimental studies on the deformation rule of the steel box type construction under the internal explosion load, of which the results suggest that the internal explosion in the box type construction can lead to a more severe damage effect than an aerial explosion, and after the deformation at the wall plate center has reached its maximum value, the deformation of the plate may have a certain amount of oscillatory rebounding. LI et al. [11] have conducted experiments for damage of the cabin explosion on the cabin structure with the warhead and analyzed the typical damage mode of the cabin grillage structure in the cabin explosion environment, of which the results suggest that the global deformation of the cabin structure under the internal explosion load of the warhead is mainly due to the damage by the shock wave. YANG et al. [12] have conducted numerical simulation of the clamped stiffened plate under three kinds of rectangular, triangular, and exponential explosive shock loads, and concluded that provided that the three kinds of loads have equal intensity, the early dynamic responses of the structures are nearly the same; as for the global damage on the structure, the rectangular pulse load causes the biggest damage, and the exponential pulse load the lowest. CHEN et al. [13] have defined the relationship between the deformation of the stiffened plate and its energy absorption under the effect of the explosive shock wave with the ratio of the dimensionless relative rigidity to deflection, and their study results provide a reference for explosion resistance and explosion venting of the warship structure. JIAO et al. [14] have proposed the value ranges of dimensionless numbers in different damage modes by describing the damage mode of the one-way stiffened plate under the shock wave with dimensionless numbers.

In Chapter "Internal Explosion" of LR Rules and Regulations for Classification of Ships [6], it is specified that if a weapon has a sufficient equivalent energy which may damage a structure with its shock load, then, the structure may be also damaged in the dynamic load assessment based on the quasi-static air pressure level. Also, it is pointed out that, when an internal explosion is taking place in the warship cabin, both the shock wave and quasi-static air pressure loads contribute to damage of the structure.

By summarizing the results of the above studies, we can find that, currently, not too many studies on the damage of the stiffened plate under the combined effect of the two loads, namely, the shock wave and quasi-static air pressure due to explosion, have been conducted. In this paper, the deformation

downloaded from www.ship-research.com

characteristics of the clamped one-way stiffened plate are simulated mainly when the load impulse is equal and load peak is equal, and the two loads are separated from each other based on the typical cabin explosion load, namely, the combined effect of the explosive shock wave and quasi-static air pressure loads. Therefore, a simulation study on the deformation characteristics of the stiffened plate can be conducted under the effect of either load and the combined effect of both loads.

1 Numerical simulation

In order to study the deformation characteristics of the cabin grillage structure under the typical cabin explosion load, we selected the one-way stiffened plate for the typical cabin grillage structure of the warship, of which the structure is shown in Fig. 1. Then, numerical simulation calculation is done with the non-linear dynamic finite element analysis program LS-DYNA, for which, the target grillage model is shown in Fig. 2.

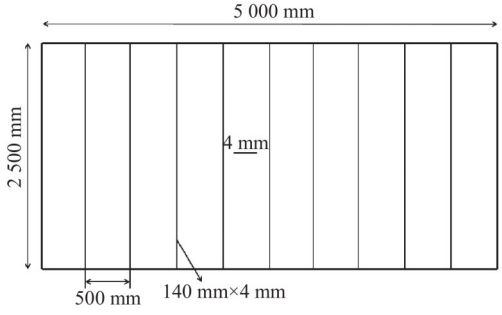

Fig. 1 Dimension structure of the stiffened plate

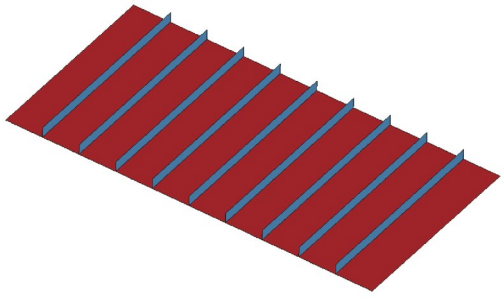

Fig. 2 Model drawing of stiffened plate

A model, l =5 000 mm, d = 2 500 mm, and height of the stiffeners h = 140 mm, has been built, with the stiffeners spaced at a = 500 mm, plate thickness H = 4 mm, and grid size 15 mm × 15 mm.

The bilinear elastic-plastic constitutive model Plastic_Kinematic is used as the material of both the face plate and stiffened structure, of which, the strain rate effect is described with the Cowper-Symonds material model:

$$\sigma_{\mathrm{d}} = \left(\sigma_0 + \frac{EE_{\mathrm{h}}}{E - E_{\mathrm{h}}}\varepsilon_{\mathrm{p}}\right)\left[1 + \left(\frac{\dot{\varepsilon}}{D}\right)^{1/n}\right] \quad (1)$$

where σ_{d} is the dynamic yield strength, σ_0 the static yield strength, E the elastic modulus, E_{h} the hardening modulus, ε_{p} the effective plastic strain, $\dot{\varepsilon}$ the equivalent plastic strain rate, and D and n are constants, generally, D= 40.4 s^{-1} and n = 5 for the mild steel. In this paper, Q235 mild steel, having density ρ=7 800 kg/m^3 and static yield strength σ_0 =235 MPa, is used. The failure criterion for maximum equivalent plastic strain, with failure strain 0.3, is applied to the material failure model.

2 Experiment validation of the numerical simulation method

In USA Military Standard UFC-3-340-02 [15], the load in a confined space is equated to two portions, of which, the 1st portion is the triangular shock wave pressure pulse without pressure rising time, and the 2nd portion the quasi-static pressure having a low peak pressure and a long pulse width. Therefore, the cabin explosion load can be equated to the shock wave load and quasi-static air pressure load. The load mode is shown in Fig. 3.

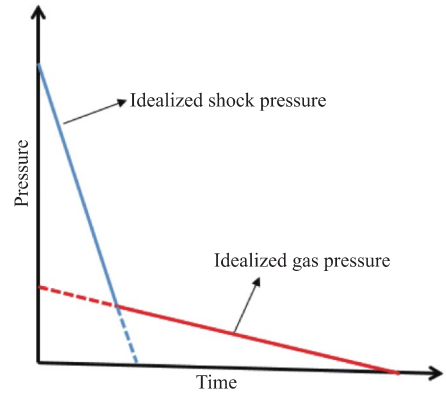

Fig. 3 The mode of explosion load in the cabin of USA standard UFC-3-340-02 [15]

The quasi-static air pressure has a smaller peak and a bigger pulse width than the shock wave, but from the aspect of the time frame, it is still a triangular shock load. Numerical simulation has been done for damage of the stiffened plate under the explosive shock load with the above simulation method and settings of the material parameters in order to validate the accuracy of the simulation software for response calculation of the structure under the shock wave load and demonstrate the applicability of the simulation method to the calculation of the triangular load. Validation has been done in the aerial explosion test as described in Ref. [16], with the test piece size 500 mm × 500 mm, 400 g TNT column charge with a size of 131.2 mm × 50.2 mm

downloaded from www.ship-research.com

and explosive distance of 148 mm. The model shell thus established is 5 mm × 5 mm in size; its boundary condition is that it is clamped all around; the fluid-structure interaction algorithm is employed and the simulation explosive is charged at the same time. The simulation results are compared with the test results [16] as shown in Fig. 4 and Fig. 5.

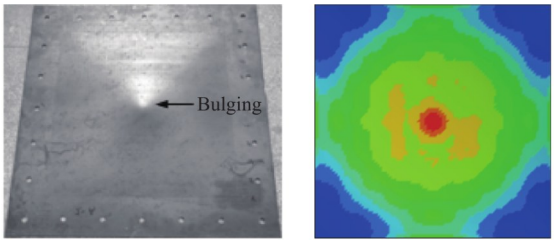

(a) Test results (b) Simulation results

Fig. 4 Comparison of test and simulation deformation modes

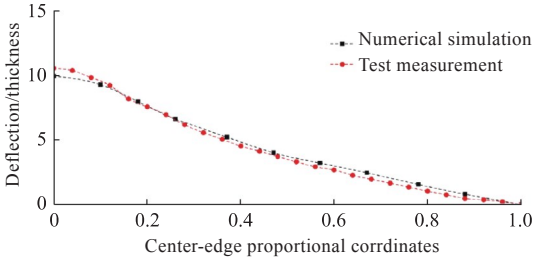

Fig. 5 Numerical comparison of deformation profile between test and simulation center line

The deformation patterns of both the test and simulation are shown in Fig. 4. It can be seen that global permanent plastic deformation has taken place on the test piece, mainly existing at the center of the square plate, and the displacement distribution resulted from the numerical simulation is in agreement with the test results. Fig. 5 provides the comparison between the deformation amount of the numerical simulation and test results. From this figure, it can be seen that the results of the numerical simulation are in good agreement with the test results. The ratio of deflection to thickness at the center of the test plate where the maximum deformation has taken place is 10.58, and that resulted from the numerical simulation is 9.98, so the error between these two values is 5.67%, less than 10%. Therefore, the simulation results meet the requirement for engineering accuracy, and it is believed that the numerical calculation method and material parameters used in this paper are rational.

3 Characteristics of the geometrical parameters of the shock wave load

In order to study the effect of the explosive shock wave load and quasi-static air pressure load on deformation of the stiffened plate, we set two kinds of loads and applied them in the form of uniform distribution as surface loads of which the parameters are listed in Table 1 and Table 2. Table 1 provides the parameters of the initial explosive shock wave load; in this table, four groups of impulses, namely, I = 2.0, 2.5, 3.0, 3.5 MPa·ms, are set, and the impulses are kept consistent by varying load action time t and load peak P_m.

Table 1 Load parameters of initial explosive impact wave

t/ms	P_m/MPa			
	I=2.0	I=2.5	I=3.0	I=3.5
0.3	13.33	16.67	20.00	23.33
0.4	10.00	12.50	15.00	17.50
0.5	8.00	10.00	12.00	14.00
0.6	6.67	8.33	10.00	11.67
0.8	5.00	6.25	7.50	8.75
1.0	4.00	5.00	6.00	7.00
1.3	3.08	3.85	4.62	5.38
1.5	2.67	3.33	4.00	4.67
2.0	2.00	2.50	3.00	3.50
4.0	1.00	1.25	1.50	1.75
6.0	0.67	0.83	1.00	1.17
8.0	0.50	0.63	0.75	0.88
10.0	0.40	0.50	0.60	0.70
14.0	0.29	0.36	0.43	0.50
18.0	0.22	0.28	0.33	0.39
20.0	0.20	0.25	0.30	0.35
24.0	0.17	0.21	0.25	0.29
30.0	0.13	0.17	0.20	0.23
50.0	0.08	0.10	0.12	0.14
80.0	0.05	0.06	0.08	0.09
100.0	0.04	0.05	0.06	0.07

In this paper, the triangular load is used to replace the initial explosive shock wave. Fig. 6 shows the schematic curves of the triangular load applied when I= 2.0 MPa·ms and load action time t = 0.3−4 ms. The load curves with other impulses given in Table 1 are similar with those in Fig. 6.

The quasi-static air pressure loads are listed in Table 2. The parameters are divided into four groups, and each group has the same load peaks P_m, respectively 0.4, 0.5, 0.6, and 0.7 MPa. With the load action time as the variable, it is found that the impulse increases gradually with an increase in the load action time.

Fig. 7 shows the schematic curves of the quasi-static air pressure loads applied. In this figure, the

downloaded from www.ship-research.com

Table 2 Parameters of quasi-static air pressure load

t/ms	I/(MPa·ms)			
	P_m=0.4	P_m=0.5	P_m=0.6	P_m=0.7
0.3	0.06	0.08	0.09	0.105
0.5	0.10	0.13	0.15	0.175
0.8	0.16	0.20	0.24	0.280
1.2	0.24	0.30	0.36	0.420
2	0.40	0.50	0.60	0.700
4.0	0.80	1.00	1.20	1.400
7.0	1.40	1.75	2.10	2.450
12.0	2.40	3.00	3.60	4.200
20.0	4.00	5.00	6.00	7.000
28.0	5.60	7.00	8.40	9.800
37.0	7.40	9.25	11.10	12.950
47.0	9.40	11.75	14.10	16.450
60.0	12.00	15.00	18.00	21.000
70.0	14.00	17.50	21.00	24.500
80.0	16.00	20.00	24.00	28.000
90.0	18.00	22.50	27.00	31.500
100.0	20.00	25.00	30.00	35.000
130.0	26.00	32.50	39.00	45.500

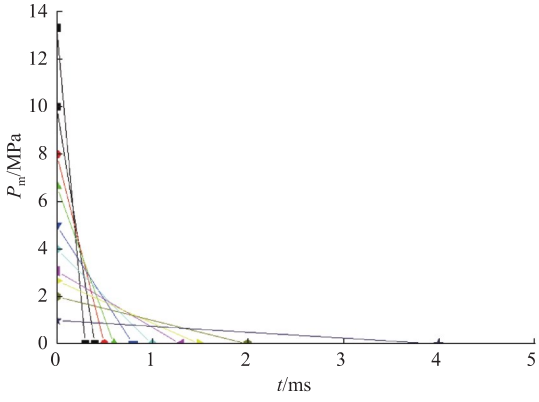

Fig. 6 Shock wave load curves (I = 2.0 MPa·ms)

load curves with impulse load peak P_m = 0.4 MPa and load action time t = 0.3−60 ms taken from Table 2 are shown. The load curves with other load peaks are similar to those in Fig. 7.

4 Numerical calculation results and analysis

4.1 Effect of the load action time on deformation of the stiffened plate under the same impulse

The simulation results when I = 2.0 MPa·ms are shown in Fig. 8. The defined global deflection value of the stiffened plate is the displacement value at the central node of the stiffened plate in direction Z. As shown in Fig. 8, with load action time t = 0.3−1.0 ms, the deflection value of the stiffened plate varies between 186.8 and 181.4 mm; with load action time t =1.3−30 ms, the global deflection of the stiffened plate varies between 177.5 and 32.0 mm; with load action time t = 50.0−100.0 ms, it varies between 23.5 and 20.0 mm.

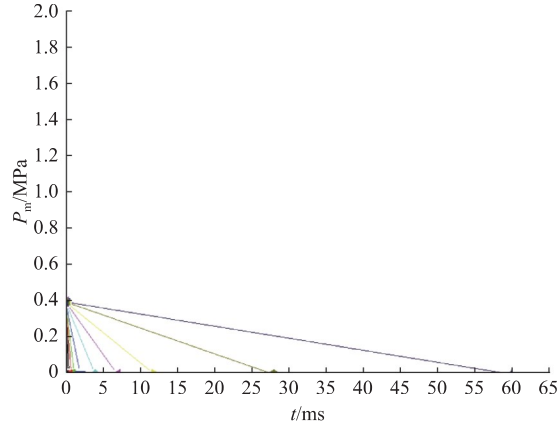

Fig. 7 Quasi-static air pressure load curves (P_m = 0.4 MPa)

Fig. 9 shows the variation of the deflection with load action time at the central position of the plate when impulse I = 2.0 MPa·ms. After the calculation, the first-order natural vibration period of this stiffened plate in the vertical direction is T = 20 ms. So it can be seen that when the load action time $t \leqslant 0.05T$ and $t \geqslant 2.5T$, the deflection of the stiffened plate varies slowly, and when $0.065T \leqslant t \leqslant 1.5T$, the deflection of the stiffened plate decreases quickly.

When I = 2.5, 3.0, or 3.5 MPa·ms, the rules for deformation of the stiffened plate with the load action time are nearly the same as those given in Fig. 8 and Fig. 9. The calculation results of the four kinds of shock wave loads are compared as shown in Fig. 10.

As can be seen from Fig. 10, when impulse I = 2.5 MPa·ms, and load action time $t \leqslant 0.075T$ or $t \geqslant$ 2.5T, the deflection of the stiffened plate varies slowly; when load action time $0.1T \leqslant t \leqslant 1.5T$, the deflection of the stiffened plate decreases slowly. When impulse I = 3.0 MPa·ms, and load action time $t \leqslant 0.075T$ or $t \geqslant 2.5T$, the deflection of the stiffened plate varies slowly; when load action time $0.1T \leqslant t \leqslant 1.5T$, the deflection of the stiffened plate decreases quickly. When impulse I = 3.5 MPa·ms, and load action time $t \leqslant 0.04T$ or $t \geqslant 2.5T$, the deflection of the stiffened plate varies slowly, and when load action time $0.04T \leqslant t \leqslant 1.5T$, the deflection of the stiffened plate decreases quickly.

From the results of the above numerical simulation, when the impulses acting on the stiffened plate

downloaded from www.ship-research.com

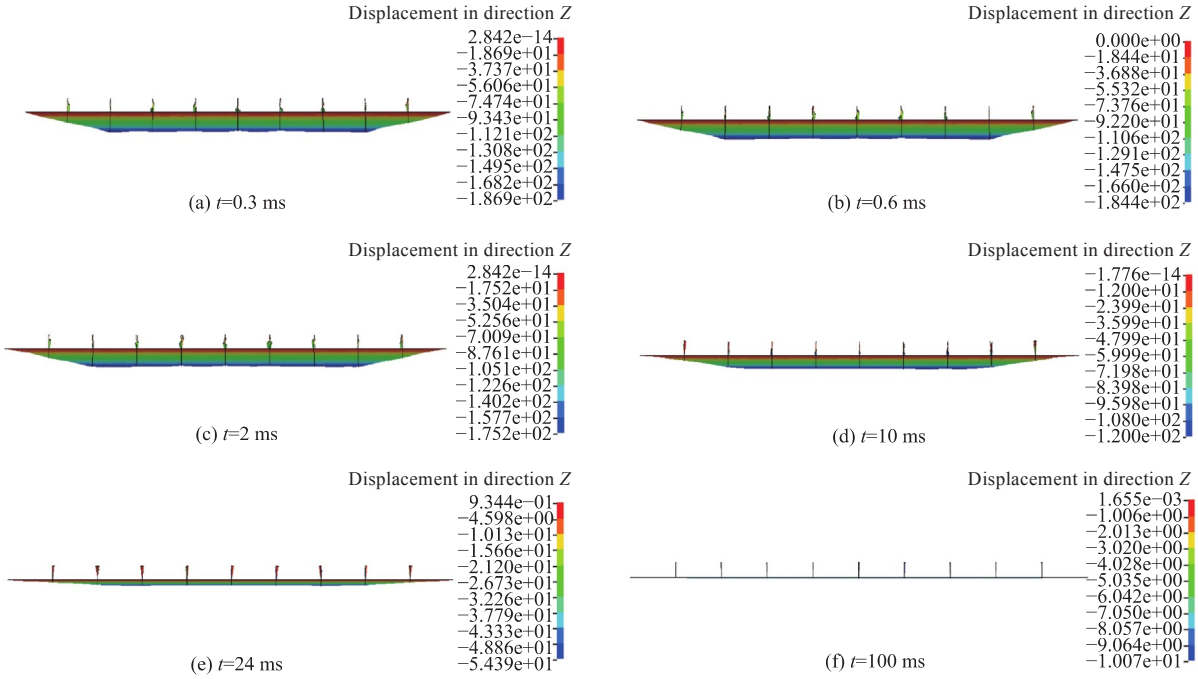

Fig. 8 Displacement contours of deformation history under shock wave (I = 2 MPa·ms)

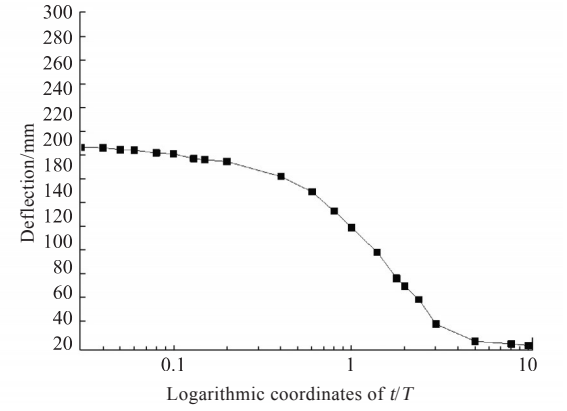

Fig. 9 The logarithmic coordinate curve of the deflection with the load time t/T

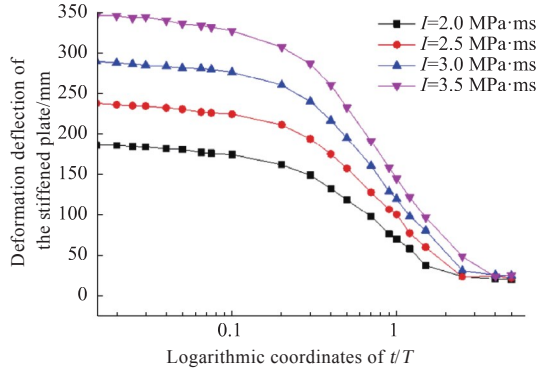

Fig. 10 Deflection calculation results under four kinds of shock wave loading strength

are equal and only a big plastic deformation has taken place, natural vibration period T of the stiffened plate may be considered; when load action time t < 0.05T, the deflection of the stiffened plate is close to the maximum value, and the final deflection tends to be stable with an increase in the load action time. Therefore, it can be believed that if the impulse is constant in the above situations, and when load action time t is less than 0.05T, the characteristics are consistent with those of the initial shock load resulted from the cabin explosion; when load action time t > 2.5T, the final maximum deflection of the stiffened plate is close to the minimum deflection, and this deflection is the final plastic deformation resulted from the shock wave. In addition, deflection due to the plastic deformation of the stiffened plate varies no longer with the extension of the load action time; when load action time t is 0.05T−2.5T, the deflection of the stiffened plate decreases gradually and varies greatly with increase in the load action time.

4.2 Effect of the load peak and load action time on deformation of the stiffened plate

Based on the situations given in Table 2, the simulation results when load peak P_m=0.4 MPa are shown in Fig. 11.

When P_m=0.4 MPa and load action time t<0.8 ms, the deformation deflection of the stiffened plate is less than 1.5 mm, so it can be believed that nearly no deformation has taken place on the stiffened plate relative to the size of the model; when load action time t is between 1.2 and 60.0 ms, the deformation of the stiffened plate increases gradually with the extension of the load action time, and

downloaded from www.ship-research.com

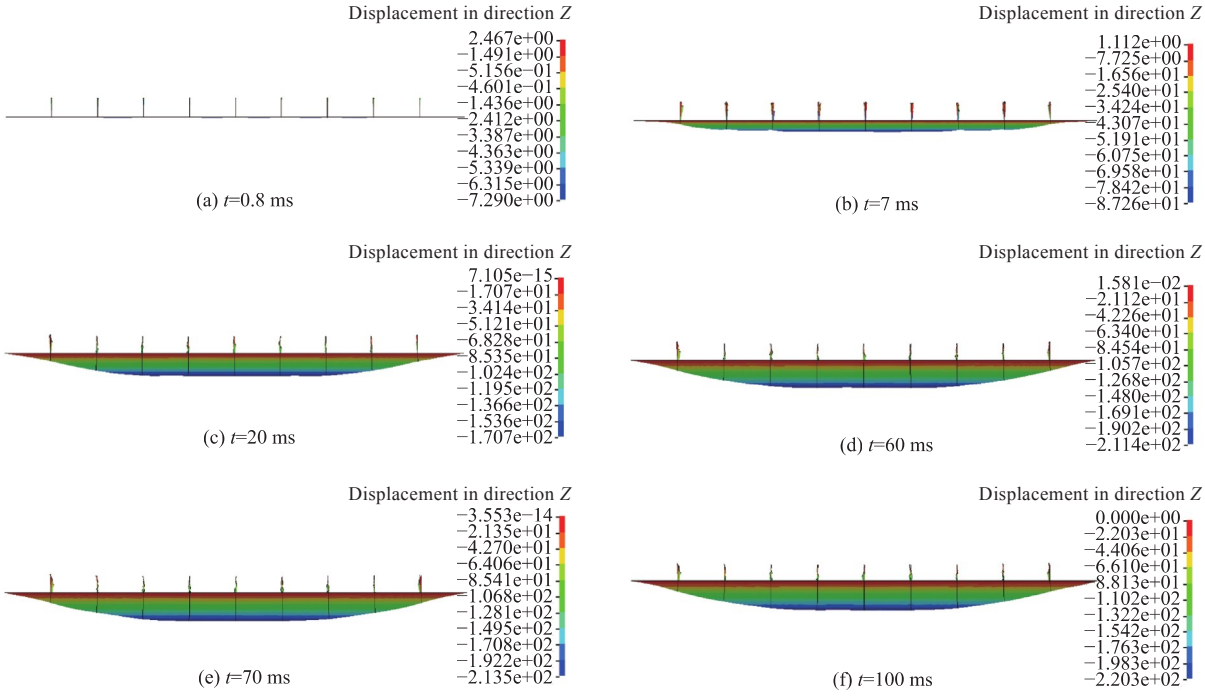

Fig. 11 Displacement contours of deformation history under quasi-static air pressure load (P_m = 0.4 MPa)

range of the deflection deformation is between 8.2 and 208.0 mm; when load action time t is longer than 70 ms or applied impulse I = 12 MPa·ms, the deflection of the stiffened plate is 212−220 mm and deflection of the stiffened plate varies little with extension of the load action time.

When P_m = 0.5, 0.6, or 0.7 MPa, the characteristics of deformation of the stiffened plate with the load action time are nearly the same as those when P_m = 0.4 MPa. The calculation results of the deflection and time under the four different loading situations are summarized as shown in Fig. 12.

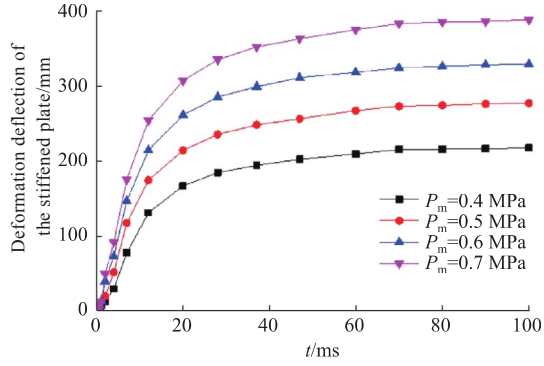

Fig. 12 Curves of deflection with time under quasi-static air pressure load

As can be seen from Fig. 12, when the load peak is low, if the load action time is long enough, it may cause a big plastic deformation on the stiffened plate. With different load peaks, when load action time t > 60 ms, the deflection of the stiffened plate reaches its maximum and it nearly varies no longer with the extension of the load action time.

So, it can be believed that saturated impulse I_s exists on the stiffened plate under different load peaks, namely, when P_m = 0.4, 0.5, 0.6, and 0.7 MPa, the saturated impulse is respectively I_s = 12, 15, 18, and 21 MPa·ms.

Therefore, it can be concluded that the load acting on the stiffened plate increases with time, and before the saturated impulse is reached, what determining the final deformation of the stiffened plate is the load action time, but after the saturated impulse is reached, it can be believed that the load action time does not affect the final deformation of the stiffened plate no longer, and what determining the final deformation of the stiffened plate is the load peak.

4.3 Characteristics of deformation of the stiffened plate under the combined effect of two kinds of loads

For the cabin explosion, the main load form is the combined effect form of the initial shock wave load and quasi-static air pressure load. The load characteristics can be studied with the characteristic experiment under the cabin explosion load with the minimum explosive charge. Fig. 13 shows the results of the shock wave pressure test under the cabin explosion [3], where, P is the load.

The model for this experiment is 1.25 m×0.75 m × 0.625 m in size, and TNT is used, with a charge mass of 33 g. As shown in Fig. 13, the action time

downloaded from www.ship-research.com

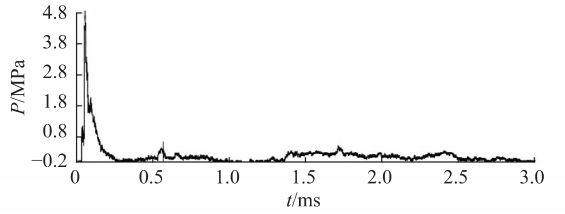

Fig. 13 Pressure history of explosive shock wave load in the cabin

of the initial shock wave is 0.25 ms and the load peak is 4.8 MPa. The quasi-static air pressure load occurs in 0.5−3.0 ms, but its load peak is 0.4 MPa, which is low. As can be seen from this experiment situation, the action time of the quasi-static air pressure load is about 10 times that of the shock wave.

As can be seen from the experiment results, the initial shock wave load nearly has the same characteristics as those under the same impulse with load action time less than $0.05T$ described in Section 4.1, and the quasi-static air pressure load nearly has the same form as the load curves described in Section 4.2 (low peak and long action time).

In order to analyze the effects of the shock wave load (peak 4.8 MPa) and quasi-static air pressure load (peak 0.4 MPa) on the deformation of the stiffened plate, we apply two kinds of loads separately or together according to the above results and based on the relation that the action time of the quasi-static air pressure load is 10 times of that of the shock wave load.

The load curves are shown in Fig. 14.

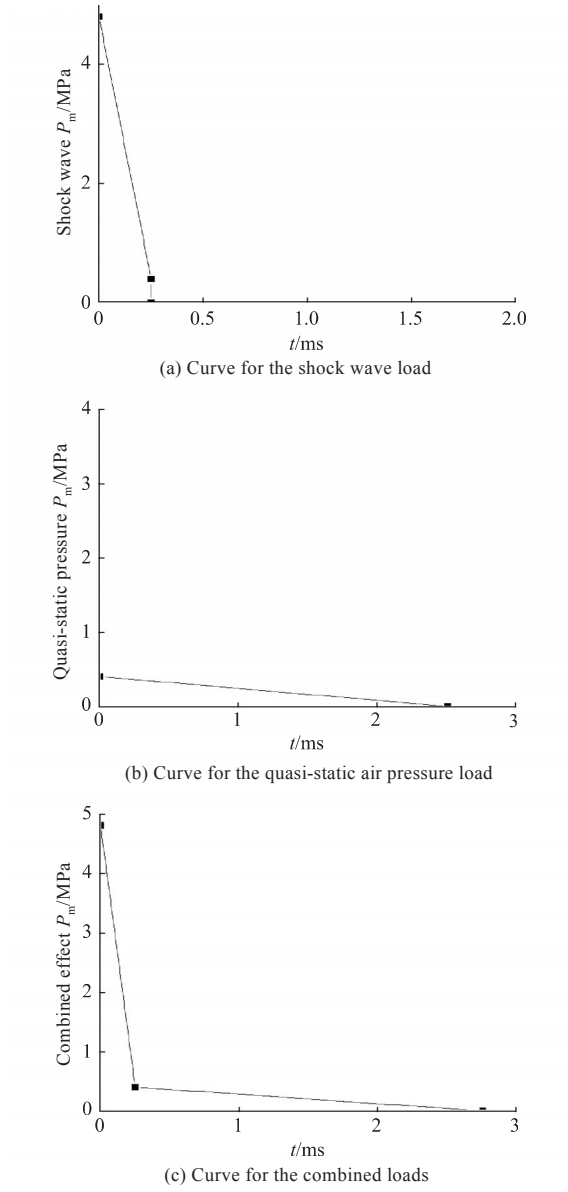

Fig. 14 Schematic diagram of load curves generation under combined action

Numerical simulation has been conducted according to the above load curves. As P_m is low, in order to obtain an obvious deformation, we set the plate thickness to 1.5 mm for the simulation, but the height of the stiffeners remains unchanged and its thickness is 2.0 mm. The simulation results are shown in Fig. 15.

As can be seen from Fig. 15, when the explosive shock wave is applied to the stiffened plate separately, the final deformation deflection of the stiffened plate is 183.6 mm; when the quasi-static air pressure is applied to the stiffened plate separately, the final deformation deflection of the stiffened plate is 85.2 mm; when the two loads are applied to the stiffened plate together, the final deformation deflection of the stiffened plate is 298.0 mm. So, it can be seen that under the cabin explosion load, what mainly contributes to the deformation of the stiffened grillage structure is the initial explosive shock load. The final deformation is not a simple superimposition of these two loads, and a combination of these two loads may aggravate the deformation of the stiffened grillage structure. In other words, the combined effect of the two loads can enhance the damage effect.

In the cabin explosion, the initial explosive shock wave has a big peak. Although its action time is short, the deformation of the stiffened plate mainly takes place in the phase in which the initial shock wave acts. After the action of the shock wave, the quasi-static air pressure continues to act, but it is lower and has a longer action time than the initial shock wave load. Thus, it also contributes to the plastic deformation of the stiffened plate as well.

downloaded from www.ship-research.com

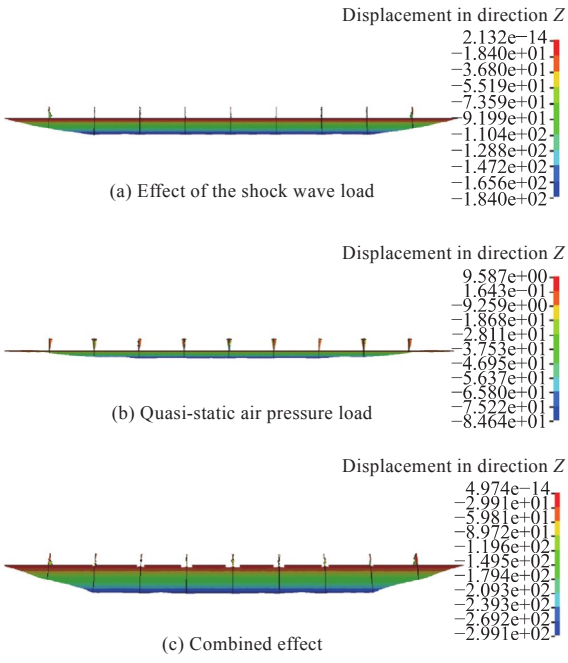

Fig. 15 Comparison of calculation results under three load forms

5 Conclusions

Numerical simulation has been conducted in view of the characteristics of the deformation of the stiffened plate under varying load action time and respectively subject to the conditions of the same impulse and same peak with the non-linear dynamic finite element analysis software LS-DYNA. The accuracy of the model built in this paper has been validated, and characteristics of the deformation of the stiffened plate under the explosive shock load, quasi-static air pressure load and combination of these two loads have been analyzed, with the following main conclusions achieved:

1) When the impulses acting on the stiffened plate are equal, only a big plastic deformation has taken place, and load action time $t < 0.05T$. This load has the same characteristics as the initial shock load in the cabin explosion, and the final deformation deflection of the stiffened plate is near the maximum value and varies little with the extension of the load action time.

2) With the same load peak, before the saturated impulse is reached, what determines the final deformation of the stiffened plate is the load action time. After the saturated impulse is reached, it can be believed that the load action time does not affect the final deformation of the stiffened plate no longer, and what determines the final deformation of the stiffened plate is the load peak.

3) Under the action of the cabin explosion load, the final deformation deflection is not a simple superimposition of these two loads, and a combination of these two loads may aggravate the deformation of the stiffened grillage structure. In other words, the combined effect of the two loads can enhance the damage effect.

References

[1] SAUVAN P E, SOCHET I, TRÉLAT S. Analysis of reflected blast wave pressure profiles in a confined room [J]. Shock Waves, 2012, 22(3): 253−264.

[2] BAKER W E. Explosion risk and its assessment [M]. ZHANG G S, trans. Beijing: Qunzhong Publishing House, 1988 (in Chinese).

[3] HOU H L, ZHU X, LI W, et al. Experimental studies on characteristics of blast loading when exploded inside ship cabin [J]. Journal of Ship Mechanics, 2010, 14(8): 901−907 (in Chinese).

[4] KONG X S, XU W Z, ZHENG C, et al. Experiment of a multi-layer protective structure under an inner explosion [J]. Journal of Ship Mechanics, 2017, 21(1): 76−89 (in Chinese).

[5] FAN Z Q, WANG W L, HUANG X F, et al. Simulation analysis on typical cabin internal explosion [J]. Engineering Blasting, 2015, 21(3): 13−17 (in Chinese).

[6] LR. Rules and regulations for classification of ships by Lloyd's register: military load code [S]. UK: Lloyd's register, 2015 (in Chinese).

[7] ZHANG Y L, SU J J, LI Z R, et al. Quasi-static pressure characteristic of TNT's internal explosion [J]. Explosion and Shock Waves, 2018, 38(6): 1429−1434 (in Chinese).

[8] JIN P G, GUO W, WANG J L, et al. Explosion pressure characteristics of TNT under closed condition [J]. Chinese Journal of Explosives & Propellants, 2013, 36 (3): 39−41 (in Chinese).

[9] YAN S W, DU M H, WANG W L, et al. Damage effect simulation of warhead inner explosion in warship cabin [J]. Journal of Naval Aeronautical and Astronautical, 2013, 28(2): 181−188 (in Chinese).

[10] YAO S J, ZHANG D, ZHENG J, et al. Experimental study of deformation of steel box subjected to internal blast loading [J]. Explosion and Shock Waves, 2017, 37 (5): 964−968 (in Chinese).

[11] LI W, ZHU X, MEI Z Y, et al. Experimental studies on damage effect of missile warhead on cabins structure under internal explosion [J]. Ship Science and Technology, 2009, 31(3): 34−37 (in Chinese).

[12] YANG C, HOU R L, LIU S F, et al. Research on dynamic responses of stiffened-plate under different blast load [J]. Journal of Wuhan University of Technology, 2010, 32(2): 56−59 (in Chinese).

[13] CHEN P Y, DUAN H, HOU H L, et al. Numerical analysis on deformation and energy absorption characteristics of stiffened plate under explosive impact loads [J]. Chinese Journal of Ship Research, 2019, 14(3): 66−

downloaded from www.ship-research.com

74 (in Chinese).
[14] JIAO L Q, HOU H L, CHEN P Y, et al. Research on dynamic response and damage characteristics of fixed supported one-way stiffened plates under blast loading [J]. Acta Armamentarii, 2019, 40(3): 592−600 (in Chinese).
[15] Structures to resist the effects of accidental explosions: UFC 3-340-02 [S]. Washington: Department of the Army, Navy, and Air Force, 2008.
[16] WU L J, ZHU X, HOU H L, et al. Simulations for damage modes of a stiffened plate subjected to closerange air-blast loading [J]. Journal of Vibration and Shock, 2013, 32(14): 77−81, 126 (in Chinese).

典型舱内爆炸载荷对加筋板的毁伤特性

焦立启[1], 张权[*2], 李茂[1], 张磊[1], 张春辉[1]
1 海军研究院,北京 100161
2 中国核动力研究设计院核反应堆系统设计技术重点实验室,四川 成都 610213

摘　要:[**目的**]为研究典型舱内爆炸载荷对加筋板的毁伤特性,将舱内爆炸载荷分为初始爆炸冲击波载荷和准静态气压载荷,利用有限元分析软件LS-DYNA开展爆炸载荷下固支单向加筋板毁伤特性的数值模拟。[**方法**]主要模拟载荷冲量相等和载荷峰值相等时固支单向加筋板的变形特性,以及加筋板分别在初始爆炸冲击波载荷、准静态气压载荷及2种载荷联合作用下的毁伤特性,并分析上述载荷作用下加筋板的变形特点。[**结果**]结果表明:当作用在加筋板上的冲量相等、载荷作用时间小于0.05倍垂向一阶自振周期时,加筋板的最终挠度值处于最大值附近;当载荷峰值相同时,存在饱和冲量值,达到饱和冲量值以后,载荷作用时间不再影响加筋板的最终变形。[**结论**]在舱内爆炸载荷作用下,加筋板的最终变形不是2种载荷作用下的简单叠加,2种载荷的联合作用会增强毁伤效果。

关键词:加筋板;舱内爆炸载荷;饱和冲量;联合作用;变形;毁伤特性

downloaded from www.ship-research.com